



# Observing $^{13}\text{C}$ labelling kinetics in $\text{CO}_2$ respired by a temperate grassland ecosystem

Ulrike Gannitzer, Rudi Schäufele and Hans Schnyder

Lehrstuhl für Grünlandlehre, Technische Universität München Am Hochanger 1, D-85350 Freising-Weihenstephan, Germany

## Summary

Author for correspondence:  
Hans Schnyder  
Tel: +49 (0) 8161 713242  
Email: schnyder@wzw.tum.de

Received: 13 March 2009

Accepted: 22 May 2009

*New Phytologist* (2009) **184**: 376–386  
doi: 10.1111/j.1469-8137.2009.02963.x

**Key words:** compartmental modelling, continuous  $^{13}\text{C}$  labelling, ecosystem respiration, grassland, online gas exchange measurements, open-top chamber, steady-state/dynamic labelling, tracer kinetics.

- The kinetic characteristics of the main sources of ecosystem respiration are quite unknown, partly because of methodological constraints. Here, we present a new open-top chamber (OTC) apparatus for continuous  $^{13}\text{C}/^{12}\text{C}$  labelling and measurement of ecosystem  $\text{CO}_2$  fluxes, and report the tracer kinetics of nighttime respiration of a temperate grassland.
- The apparatus includes four dynamic flow-through OTCs, a unit mixing  $\text{CO}_2$ -free air with  $^{13}\text{C}$ -depleted  $\text{CO}_2$ , and a  $\text{CO}_2$  analyser and an online isotope ratio mass spectrometer.
- The concentration ( $367 \pm 6.5 \mu\text{mol mol}^{-1}$ ) and carbon isotopic composition,  $\delta^{13}\text{C}$ , ( $-46.9 \pm 0.4\text{‰}$ ) of  $\text{CO}_2$  in the OTCs were stable during photosynthesis as a result of high air throughflux and minimal incursion through the buffered vent. Soil  $\text{CO}_2$  efflux was not affected by pressure effects during respiration measurements. The labelling kinetics of respiratory  $\text{CO}_2$  measured in the field agreed with that of excised soil + vegetation blocks measured in a laboratory-based system. The kinetics fitted a two-source system ( $r^2 = 0.97$ ), with a rapidly labelled source (half-life 2.6 d) supplying 48% of respiration, and the other source (52%) releasing no tracer during 14 d of labelling.
- Of the two sources supplying ecosystem respiration, one was closely connected to current photosynthesis ( $\approx$  autotrophic respiration) and the other was provided by decomposition of structural plant biomass ( $\approx$  heterotrophic respiration).

## Introduction

This work is concerned with the kinetics of substrate supply to ecosystem respiration in a temperate grassland system. In grasslands, as in other ecosystems, most of the carbon (C) fixed in photosynthesis is eventually returned to the atmosphere by way of autotrophic or heterotrophic respiration. However, there is an enormous variation in the time lag between C fixation and release. For example, if current photosynthate is used in root respiration, then the residence time of C in the system is short (hours to days); but if C is incorporated in structural compounds then the residence time is long (months to centuries) (Högberg & Read, 2006). So, the residence time of C in the biosphere is a function of allocation. Knowledge of (respiratory substrate) C allocation and associated pool kinetics is important for understanding C cycling and ecosystem C storage (Trumbore, 2006).

Manipulation and monitoring of the isotopic composition of assimilated C can be used to trace C on its way through an ecosystem with no (or minimal) disturbance of photosynthesis,

allocation and respiration. Turnover of respiratory C pools has mainly been studied in controlled environments at different levels of biological integration: leaves (Nogues *et al.*, 2004), root and shoot (Lehmeier *et al.*, 2008), whole plants (Ryle *et al.*, 1976), and mesocosms (Schnyder *et al.*, 2003). However, field labelling studies are essential to allow mechanisms detected in artificial environments to be assessed in natural conditions and at the ecosystem level. In field studies, the residence time of C or respiratory labelling kinetics (the time course of tracer in respired  $\text{CO}_2$ ) has been investigated using pulse-chase tracer techniques in forest (Carbone *et al.*, 2007; Högberg *et al.*, 2008) and grassland ecosystems (Ostle *et al.*, 2000; Johnson *et al.*, 2002; Carbone & Trumbore, 2007; Bahn *et al.*, 2009). Pulse labelling causes strong labelling of rapidly turned over pools, but weak labelling of slowly turned over pools (Geiger, 1980; Meharg, 1994), impeding the assessment of the contribution of the slow pools to respiration. Continuous labelling (also termed 'dynamic labelling' (Ratcliffe & Shachar-Hill, 2006), or – more classically – 'steady-state labelling' (Geiger, 1980) in plant biology literature) avoids this complication: the amount of tracer in

respired  $\text{CO}_2$  increases until, eventually, all substrate pools of respiration have reached isotopic equilibrium. The kinetics of this increase reflects the functional properties of the pool system supplying respiration (the number and arrangement of pools, and the size, turnover rate and contribution of individual pools to the total respiratory flux), which can be uncovered by compartmental analysis (Atkins, 1969; Jacquez, 1996).

To our knowledge, no technique for continuous labelling at ambient  $\text{CO}_2$  in the field has yet been described. For this, plants must be exposed to an atmosphere with a C isotopic composition of  $\text{CO}_2$  that is different from that under natural conditions but constant and homogeneous during daylight hours. For labelling at ambient  $\text{CO}_2$ , manipulation of the isotopic composition can be achieved by enclosing the ecosystem in an open chamber (more exactly termed a steady-state flow-through system; see Livingston & Hutchinson, 1995), flushed with air containing  $\text{CO}_2$  of the desired C isotopic composition. The technique should ensure that the concentration and isotopic composition of  $\text{CO}_2$  in the chamber headspace are not significantly altered by photosynthesis and respiration and associated isotopic discrimination. Ideally, climatic conditions inside the chamber should not differ from natural conditions.

The most obvious method for nondestructive, *in situ* detection of tracer in respired  $\text{CO}_2$  is the analysis of gas exchange in an open chamber system, in combination with online C isotope analysis. In such a system, the dark respiration rate is quantified as the difference between chamber inlet and outlet  $\text{CO}_2$  fluxes. Analogously, the isotopic composition of respired  $\text{CO}_2$  is assessed from the isotopic mass balance of inlet and outlet  $\text{CO}_2$  fluxes. Such measurements are susceptible to artefacts such as ambient air incursions and pressure effects. To minimize incursion, Baldocchi *et al.* (1989) recommended decreasing the size of the chamber opening below the length scale of turbulence elements and increasing the velocity of air exiting through the top ( $v_{\text{exit}}$ ) to oppose the entraining ambient

air. However, increasing  $v_{\text{exit}}$  can cause pressure effects which reduce soil  $\text{CO}_2$  efflux considerably: overpressure of  $< 1$  Pa can suppress soil  $\text{CO}_2$  efflux by  $> 50\%$  (Fang & Moncrieff, 1998; Lund *et al.*, 1999; see also Kanemasu *et al.*, 1974). Thus, chamber design and operating conditions must minimize the conflict between air incursion and pressure artefacts.

In this paper we present a new system, based on open-top chambers (OTCs), for the continuous application of a  $^{13}\text{CO}_2/^{12}\text{CO}_2$  tracer on grassland ecosystems and the quasi-continuous online measurement of the tracer in ecosystem respiration in the field. To assess its performance, we investigated (1) the constancy and homogeneity of the concentration and isotopic composition of  $\text{CO}_2$  inside the chambers, (2) effects of chamber design and operating conditions on air incursion and on the accuracy of measurement of respiratory  $\text{CO}_2$ , including pressure effects, and (3) environmental conditions inside the OTCs. Then, (4) we measured the tracer kinetics of respiration in a temperate grassland ecosystem during a 16-d-long labelling interval and (5) compared these field respiration measurements with laboratory-based (reference) measurements of excised soil + vegetation blocks. Finally, (6) we analysed and interpreted the tracer kinetics with a simple compartmental model.

## Materials and Methods

### Open-top chamber system for labelling and respiration measurement

The chamber system, schematically shown in Fig. 1, consisted of three main parts: (1) four OTCs; (2) a unit supplying air of the desired  $\text{CO}_2$  concentration and isotopic composition; and (3) the gas exchange measurement unit, including sample selection, an infrared gas analyser for  $\text{CO}_2$  and water vapour concentration analysis, and a continuous-flow isotope-ratio mass spectrometer for analysis of  $^{13}\text{CO}_2$ .

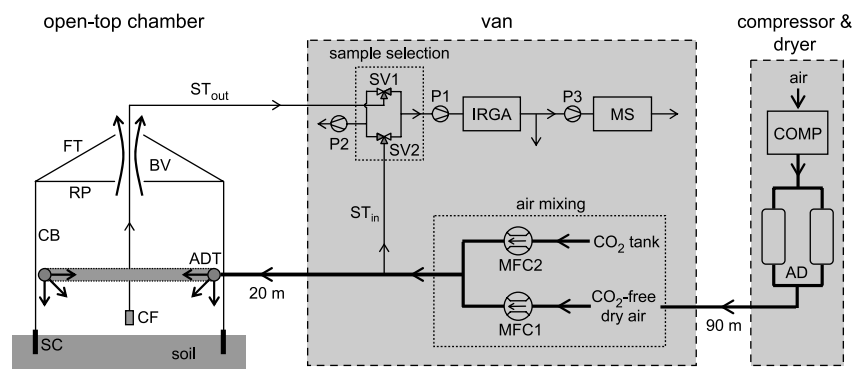


**Fig. 1** Schematic diagram of the chamber system consisting of an open-top chamber (CB, chamber body; RP, removable plate; FT, frustum top; BV, buffer volume; SC, soil collar), air supply unit (COMP, screw compressor; AD, adsorption dryer; MFC1, mass flow controller for air flow; MFC2, mass flow controller for  $\text{CO}_2$  flow; ADT, air distribution tube) and gas exchange observation unit ( $\text{ST}_{\text{in}}/\text{ST}_{\text{out}}$ , sampling tubes for chamber inlet/outlet; CF, coarse filter; SV1 and SV2, three-way solenoid valves for sample selection; P1, sample pump; P2, bypass pump; IRGA, infrared gas analyser; P3, mass spectrometer sample air pump; MS, gas chromatographic column and isotope ratio mass spectrometer). Thick lines indicate flow to/through the chamber, and thin lines indicate sample air flow. For clarity only one (out of four) open-top chamber with its air mixing system and sample selection valves is shown. All chambers had their own gas mixing unit, and gas supply and sampling air lines.

The chambers consisted of clear acrylic glass (Plexiglas XT 20070, 4 mm thick; Röhm Degussa, Darmstadt, Germany; for transparency to photosynthetic active radiation see 'Characterization of chamber properties' below). The chamber body had a cylindrical shape, based on an octagon of 100 cm diameter, resulting in a chamber base area,  $A_{\text{chamber}}$ , of 0.83 m<sup>2</sup>. The chamber body height was 80 cm, and the volume 660 l. A removable horizontal plate with a hole in the middle was placed on top of the cylindrical body. In addition, a removable open frustrum with an angle of 30° was placed on the cylinder. In the final configuration the diameter of the opening in both top parts could be adjusted between 6.5 and 32 cm, corresponding to 0.4–10% of the chamber base area.

To separate the enclosed part of the ecosystem from the surrounding environment, the chamber was placed on a 15-cm-high stainless steel collar, which was forced *c.* 12 cm into the soil. A water-filled channel on top of the collar provided sealing between the collar and the chamber body. Some of the chamber tests were performed with the chamber bottom sealed with a plastic or stainless-steel plate to exclude soil and vegetation signals.

To supply the chambers with air of the desired CO<sub>2</sub> concentration and isotopic composition, the principle introduced by Deléens *et al.* (1983) was followed: CO<sub>2</sub>-free dry air was generated at a rate of *c.* 3200 standard litres per minute (SLPM) using a screw compressor (A50-H8; Babatz, Bad Wimpfen, Germany) which fed an adsorption dryer (KEN 3100; Zander, Essen, Germany). The CO<sub>2</sub>-free dry air was conveyed to a mixing unit, housed 90 m away in an air-conditioned van, via a polyethylene (PE) tube which was buried in the soil at a depth of 70 cm. Each chamber was equipped with a separate mixing unit, consisting of one mass flow controller (Bronkhorst Hi-Tec, Ruurlo, the Netherlands; 0–1000 SLPM), which controlled the flow of CO<sub>2</sub>-free air, and another mass flow controller (Millipore, Billerica, MA, USA; 0–1 SLPM), which controlled the amount of CO<sub>2</sub> added to the air stream from a high-pressure cylinder. Maximum air flow per chamber was 800 SLPM when all four chambers were operated. The chambers were connected to their mixing units via flexible tubes (PVC fabric tubes; length ≤ 20 m; inner diameter 32 mm). Air distribution in the OTC was achieved with a circular tube (circle diameter 93 cm; tube inner diameter 32 mm) mounted at *c.* 30 cm height inside the chamber. The tube contained 46 holes (8 mm diameter) which directed the air downwards, inwards and diagonally downwards/inwards. To avoid excessive warming of the air inside the OTCs as a result of the glasshouse effect, the air supplied to the OTCs was cooled by burying the tube upstream of the mixing unit in the soil, expanding the air from 0.7 MPa to ambient air pressure in the mixing unit, and thermally isolating the downstream air supply tubes. Transpiration by the canopy and evaporation by the soil inside the OTC contributed further cooling.

For analysis of CO<sub>2</sub>, the chamber inlet was sampled with a teflon (polytetrafluoroethylene, PTFE) tube which diverged

from the chamber's air supply immediately after the mixing unit. Outlet air was sampled inside the chamber using a PTFE tube which was equipped with a coarse filter. Each chamber was equipped with its own sampling tubes. The sample tubes of the chamber inlets and outlets were connected to a system of three-way solenoid valves which allowed selection of one (out of a total of eight; two per chamber) sample tube for analysis, while the other tubes were flushed. This enabled rapid sequential analysis of all eight sample lines with one set of analysers. Sample air from the selected line was drawn with a membrane pump at approx. 1.6 SLPM and passed on to an infrared gas analyser (IRGA; LI 7000; Li-Cor, Lincoln, NE, USA) and continuous-flow isotope-ratio mass spectrometer (Delta Plus Advantage; Thermo Electron, Bremen, Germany) interfaced with a gas chromatographic column (Gasbench II; Thermo Electron) (Schnyder *et al.*, 2004). Carbon isotopic compositions are presented as  $\delta^{13}\text{C} = R_{\text{sample}}/R_{\text{standard}} - 1$ , where  $R_{\text{sample}}$  and  $R_{\text{standard}}$  are the <sup>13</sup>C/<sup>12</sup>C ratios in the sample and in the international VPDB standard. All mass spectrometric measurements were corrected for linearity effects (i.e. dependence of the raw  $\delta^{13}\text{C}$  value on the actual CO<sub>2</sub> concentration) according to measurements of a laboratory standard CO<sub>2</sub>, mixed in CO<sub>2</sub>-free air at different concentrations. The sample selection unit and the measurement instrumentation were placed in a temperature-controlled van.

Each chamber was equipped with a set of sensors for environmental conditions, including air temperature/relative humidity (1400-104; Li-Cor), soil temperature (1400-103; Li-Cor) and photosynthetic photon flux density (PPFD) (LI-190SZ quantum sensor interfaced with photomultiplier MV-100; Li-Cor). Each air temperature/relative humidity sensor was mounted in a double-walled, ventilated housing. The sensors agreed within 0.2°C (SD) air temperature and 0.5% (SD) relative humidity when exposed to the same environment. PPFD sensors were installed horizontally and agreed within 11 μmol m<sup>-2</sup> s<sup>-1</sup> (SD).

For central control of the system and data acquisition, the flow controllers, the environmental conditions sensors, the sample selection valves and the IRGA were connected to a PC via Field Point communication modules (National Instruments, Austin, TX, USA). Setting of flow rates and automated sample selection as well as data logging for the selected sample line on a 1-s basis were performed with custom-built software (Walz, Effeltrich, Germany). As the mass spectrometer was equipped with a separate PC, synchronization of mass spectrometer sampling intervals with sample selection times was carried out by means of a trigger.

All measurements were carried out in a temperate humid grassland at Grünschaige Grassland Research Station (Schnyder *et al.*, 2006). The chamber system was placed in the middle of paddock number 8. An eddy-covariance system was located near the van and logged 3D wind speed (CSAT3; Campbell Scientific, Logan, UT, USA) and CO<sub>2</sub> concentration (LI 7500; Li-Cor) at 1.5 m height (H. Schnyder, unpublished data).

## Characterization of chamber properties

**Mixing of chamber air** To quantify the distribution of incoming air within the chamber, an empty OTC (opening size 0.4% of chamber base area) with an impermeable base was flushed with CO<sub>2</sub>-free dry air at 100 SLPM (which was close to the lower limit of adjustable air flows). Then, the CO<sub>2</sub> concentration in the incoming air was suddenly increased to 1000 µmol mol<sup>-1</sup> and, after nearly reaching this value in the chamber air, suddenly decreased back to 0 µmol mol<sup>-1</sup>. The change of CO<sub>2</sub> concentration following the concentration switches was tracked at 12 positions distributed horizontally and vertically over the chamber cross-section (see Supporting Information, Fig. S2) for 25–30 min. This was done by installing the chamber outlet sampling tube and taking IRGA readings, consecutively at each of the positions.

**Ambient air incursion** An empty OTC with an impermeable base was also used to quantify the amount of ambient air blown into the chamber through the open top. For this, the chamber was continuously flushed with CO<sub>2</sub>-free dry air, and the CO<sub>2</sub> concentration inside (25 cm sampling height) and outside the chamber was monitored. The ratio of ambient air to total air inside the chamber ( $\text{air}_{\text{amb}}/\text{air}_{\text{chamber}}$ ) was given by the ratio of CO<sub>2</sub> concentration inside the chamber to CO<sub>2</sub> concentration in ambient air.

**Pressure effects on soil CO<sub>2</sub> efflux** The disturbance of soil CO<sub>2</sub> efflux by chamber pressure effects was investigated with an OTC placed on a grassland ecosystem section from which the aboveground biomass had been completely removed. All observations were completed within 6 h after shoot removal. The chamber, set up with different top opening sizes, was flushed with air at different flow rates, providing a range of chamber exit velocities,  $v_{\text{exit}}$ . Soil CO<sub>2</sub> efflux rate was calculated from the CO<sub>2</sub> concentration difference between chamber inlet and outlet, and the rate of air flow through the OTC, according to Eqn 1. Simultaneously with CO<sub>2</sub> efflux rate, the pressure difference between the inside and outside of the OTC,  $p_{\text{diff}} = p_{\text{inside}} - p_{\text{outside}}$ , was monitored by connecting the sample port of a differential pressure sensor (LP8000; Druck Limited, Leicester, UK) to the chamber inside via a tube, while the sensor's reference port was exposed to ambient air.

**Light transmission** Light transmission of the OTC was quantified with PPF sensors mounted at eight different places spread over the chamber cross-section at plant canopy height and a reference sensor mounted outside the chamber. Light attenuation by the OTC occurred as a result of reflection by the chamber wall material and as a result of partial shading caused by installations such as air supply and sampling tubes. Mean light transmission of the chamber system was 82% in sunny conditions.

## Protocol of labelling experiment

In May 2007, a 16-d-long labelling experiment was performed on a part of the pasture that had recovered from grazing for *c.* 2 wk. For site conditions see Schnyder *et al.* (2006). 5–10 d before the start of labelling, soil collars were installed at 10 selected sites. The vegetation at all sites was dominated by *Lolium perenne* L., *Poa pratensis* L., *Trifolium repens* L. and *Taraxacum officinale* L. and had a mean canopy height of 6–7 cm. Tracer was applied during daytime hours and ecosystem respiration was measured online in the field during nighttime hours. The first respiration measurements were made in the night before the start of the labelling experiment, to obtain the isotopic signature of respiration from the nonlabelled ecosystem. Measurements were continued every night for the entire duration of labelling. Sites were labelled individually for periods of 1, 2, 4, 8 or 16 d, with two replications each. All labelling was performed within a 16-d period, using four OTCs. Two OTCs were used to label two sites for the entire 16-d-long period, and the other two OTCs rotated between sites for the shorter labelling durations. This sampling scheme was chosen to allow direct comparison of (nondestructive) *in situ* and reference measurements (which required the sampling of the labelled vegetation; see 'Reference measurements' below).

**Daytime labelling** Labelling was started in the early morning by placing an OTC (opening size 1% of chamber base area) on a soil collar. For the desired number of labelling days, the chamber was flushed from 05:30 to 21:00 h (local time) with 760 SLPM dry air containing 391 µmol mol<sup>-1</sup> CO<sub>2</sub> at the chamber inlet. The chambers were supplied with CO<sub>2</sub> depleted in <sup>13</sup>C ( $\delta^{13}\text{C} = -48.6\text{‰}$ ) compared with ambient air CO<sub>2</sub> ( $\delta^{13}\text{C} = -8.5\text{‰}$ ). Each morning at sunrise, each chamber was watered with the equivalent of the previous day's evaporation plus an extra 20% to account for run-off (5–10 mm in total). Sensors for air temperature/relative humidity and soil temperature (approx. 5 cm depth) were placed inside the OTC, while PPF sensors were placed outside. The air sampling tubes inside each chamber were installed at 20–25 cm above the canopy.

**Nighttime respiration measurements** During darkness (between 23:30 and 05:30 h local time) respired CO<sub>2</sub> was analysed by measuring the gas exchange of each OTC, in combination with C isotope analysis of CO<sub>2</sub>. For these measurements, the air flow through the chamber was kept at 100 SLPM (compared with 760 SLPM during daytime labelling). The CO<sub>2</sub> concentration at the chamber inlet was maintained at 388 µmol mol<sup>-1</sup> and  $\delta^{13}\text{C}$  at  $-48.6\text{‰}$  throughout the nighttime respiration measurements, which is the same value as during daytime labelling. To allow for equilibration after reducing the air flow, chambers were flushed for at least 1 h before the first measurements were taken. The net CO<sub>2</sub> flux,  $F_{\text{resp}}$ , and the <sup>13</sup>C signature of the net flux,  $\delta_{\text{resp}}$ , were calculated from

the change in CO<sub>2</sub> concentration and δ<sup>13</sup>C between chamber inlet and outlet, according to mass balance equations:

$$F_{\text{resp}} = \frac{F_{\text{air}}}{V_{\text{mol}} A_{\text{chamber}}} (C_{\text{out}} - C_{\text{in}}) \quad \text{Eqn 1}$$

$$\delta_{\text{resp}} = \frac{\delta_{\text{out}} C_{\text{out}} - \delta_{\text{in}} C_{\text{in}}}{C_{\text{out}} - C_{\text{in}}} \quad \text{Eqn 2}$$

( $F_{\text{air}}$ , the air flow through the chamber (corresponding to 100 SLPM);  $A_{\text{chamber}}$ , the chamber base area;  $V_{\text{mol}}$ , the molar volume of gases (22.4 l mol<sup>-1</sup>);  $C_{\text{in}}$  and  $C_{\text{out}}$ , the CO<sub>2</sub> concentrations at chamber inlet and outlet, respectively;  $\delta_{\text{in}}$  and  $\delta_{\text{out}}$ , the respective δ<sup>13</sup>C values.)

The fraction of newly assimilated (labelled) carbon in respired CO<sub>2</sub>,  $f_{\text{new}}$ , was calculated from  $\delta_{\text{resp}}$  according to mass balance considerations as

$$f_{\text{new}} = \frac{\delta_{\text{resp}} - \delta_{\text{old}}}{\delta_{\text{new}} - \delta_{\text{old}}} \quad \text{Eqn 3}$$

( $\delta_{\text{old}}$  and  $\delta_{\text{new}}$ , the <sup>13</sup>C signatures of CO<sub>2</sub> respired by the nonlabelled ecosystem (measured in the night before the beginning of the labelling experiment) and by the labelled ecosystem at the new isotopic equilibrium, respectively.) As the labelling duration was too short to achieve isotopic equilibrium,  $\delta_{\text{new}}$  was estimated from C isotope discrimination, Δ, and the measured δ<sup>13</sup>C of CO<sub>2</sub> inside the OTC during daytime tracer uptake,  $\delta_{\text{out}}$  (daytime), as in Schnyder *et al.* (2003):

$$\delta_{\text{new}} = \frac{\delta_{\text{out}}(\text{daytime}) - \Delta}{1 + \Delta} \quad \text{Eqn 4}$$

Δ was obtained from the measurements of the unlabelled system as

$$\Delta = \frac{\delta_{\text{amb}} - \delta_{\text{old}}}{1 + \delta_{\text{old}}} \quad \text{Eqn 5}$$

( $\delta_{\text{amb}}$ , the C isotope composition of ambient air at the site during daytime hours.) This estimation was based on the assumption that discrimination was not altered by the conditions inside the OTC, so that discrimination was the same for the labelled and nonlabelled fractions of respired CO<sub>2</sub>.

**Reference measurements** A laboratory-based open <sup>13</sup>CO<sub>2</sub>/<sup>12</sup>CO<sub>2</sub> gas exchange system (Löttscher *et al.*, 2004) was used for reference measurements of the isotopic composition of ecosystem respiration. For that purpose, four soil + vegetation blocks of 15 cm diameter and 10–11 cm soil depth were excised from each labelled site immediately after the termination of labelling and on-site respiration measurements. The laboratory-based system of Löttscher *et al.* (2004) was adapted with a new cuvette (Fig. S1). Ecosystem respiration was measured by placing the excised soil + vegetation blocks in the cuvette volume of the system, completely enclosing the block in the cuvette. The four cuvettes (one for each

soil + vegetation block) were placed in a plant growth cabinet controlled at 18°C, the soil temperature of the labelling site at the beginning of the experiment. Cuvettes were operated in the open mode by flushing air through each cuvette, and measuring the concentration and isotopic composition of respired CO<sub>2</sub> in the inlet and outlet air fluxes.

## Results

### Chamber performance

**Mixing of chamber air** The mixing characteristics of OTCs were analysed by following the kinetics of CO<sub>2</sub> concentration change in chamber headspace air following CO<sub>2</sub> concentration switches in the inlet air flow. The increases and decreases of CO<sub>2</sub> concentration in the chamber headspace fitted exponential curves ( $r^2 > 0.999$ ), indicating near-instantaneous mixing of incoming air with chamber headspace air. Half-lives at the different positions in the chamber varied very little, and ranged between 242 and 254 s (Fig. S2). The longest half-lives were observed at the chamber bottom, the shortest ones close to the chamber top.

In the case of instantaneous mixing, the half-life depends only on the rate of air flow through the chamber and the chamber volume. As a result of the glasshouse effect, air inside the chamber is heated up, causing thermal expansion of the air volume. With chamber air temperatures of 20–30°C, the theoretical half-life ranged between 230 and 240 s. The longer half-life at the chamber bottom (compared with the upper chamber section) was related to heating of air between entering the chamber close to the bottom and leaving through the open top.

**Ambient air incursion** Chamber designs with and without the plate mounted below the frustrum top of the OTC (RP in Fig. 1) were investigated with respect to the effect on air incursion, assessed by the ratio  $\text{air}_{\text{amb}}/\text{air}_{\text{chamber}}$ . Other chamber parameters and operating conditions were held the same as during respiration measurements (Table 1). CO<sub>2</sub> concentration data were averaged over the half-life of chamber air.

Ambient air incursion into the chamber was reduced by a factor of nearly 40 when the plate was mounted. Thus, the volume between the plate and the frustrum top acted as an effective buffer between the chamber body and ambient air. Accordingly, investigations of the effect of wind speed on ambient air incursion were performed with the plate mounted, as during respiration measurements. On average,  $\text{air}_{\text{amb}}/\text{air}_{\text{chamber}}$  was *c.* 0.0015 for wind speeds above 2 m s<sup>-1</sup> and lower for lower wind speeds (Fig. 2). In 95% of the measurements  $\text{air}_{\text{amb}}/\text{air}_{\text{chamber}}$  was below 0.0026. For wind speeds below 2 m s<sup>-1</sup> this fraction was even lower (Fig. 2).

**Disturbance of soil CO<sub>2</sub> efflux** The pressure difference between the outside and inside of the OTC did not increase significantly

**Table 1** Comparison of open-top chamber with and without a plate mounted at the chamber top below the frustrum with respect to ambient air incursion ( $\text{air}_{\text{amb}}/\text{air}_{\text{chamber}}$ )

Chamber parameters	$v_{\text{exit}}$ ( $\text{m s}^{-1}$ )	0.2
	Air flow (SLPM)	100
	Opening (% of base area)	1
$\text{air}_{\text{amb}}/\text{air}_{\text{chamber}}$	Chamber without plate	$0.065 \pm 0.020$ ( $n = 3$ )
	Chamber with plate	$0.0018 \pm 0.0007$ ( $n = 71$ )
Ratio	(without plate)/(with plate)	37.1

$\text{air}_{\text{amb}}/\text{air}_{\text{chamber}}$ , ratio of ambient air to total air inside the chamber (mean  $\pm$  SD of measurements at windspeed between 2 and 4  $\text{m s}^{-1}$ ); SLPM, standard litres per minute;  $v_{\text{exit}}$ , the velocity of air exiting through the top.

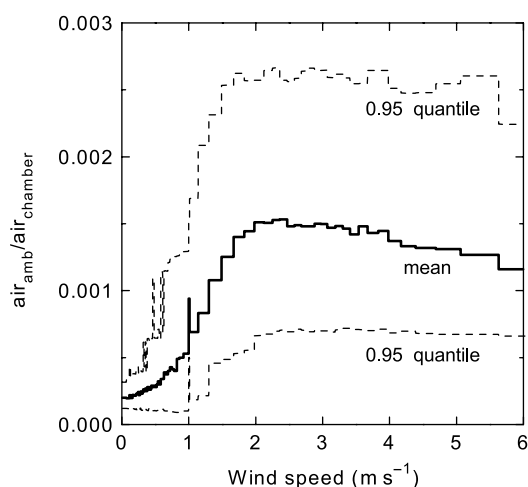


**Fig. 2** Influence of wind speed on the ratio  $\text{air}_{\text{amb}}/\text{air}_{\text{chamber}}$  for the chamber set-up used during respiration measurements (opening size 1% of base area; air flow 100  $\text{l min}^{-1}$ ; chamber with removable plate; see Fig. 1). Each step represents the mean (solid line) and 0.05 and 0.95 quantiles (dashed lines), respectively, of 1000 measurements (1-s averages) falling into the wind speed interval indicated by the width of the horizontal step.

at exit velocities,  $v_{\text{exit}} < 0.2 \text{ m s}^{-1}$  ( $P = 0.16$ ; Fig. 3a). However, beyond  $0.2 \text{ m s}^{-1}$ , overpressure inside the chamber increased quadratically with increasing  $v_{\text{exit}}$  (Fig. 3b). Soil  $\text{CO}_2$  efflux, measured simultaneously with pressure difference, also showed no significant relationship with  $v_{\text{exit}}$  if  $v_{\text{exit}}$  was  $< 0.2 \text{ m s}^{-1}$  ( $P = 0.30$ ; Fig. 3c). However, soil  $\text{CO}_2$  efflux decreased when  $v_{\text{exit}}$  increased between 0.2 and 2  $\text{m s}^{-1}$ . Increases of  $v_{\text{exit}}$  beyond 2  $\text{m s}^{-1}$  caused no further decrease of soil  $\text{CO}_2$  efflux (Fig. 3d).

**Climatic conditions inside the chambers** Daytime air temperature inside the OTCs was nearly identical to ambient air temperature on average over the whole labelling experiment, with a root mean squared difference (RMSE) of  $2.7^\circ\text{C}$  (based on  $\sim 10$ -min averages, recorded in each of the four OTCs once per hour; see Fig. S3a). Nighttime air temperature during respiration measurements was  $0.3^\circ\text{C}$  lower on average inside the chambers than outside, with an RMSE of  $1.2^\circ\text{C}$ . Even on sunny days (Fig. S3c), maximum temperature inside the chambers did not exceed  $28^\circ\text{C}$  while ambient air temperature reached  $30^\circ\text{C}$ .

All the humidity in the chamber air originated from evapotranspiration inside the chamber, as the air entering the chambers was dry. Relative humidity (Fig. S3b) in the chambers was  $c. 45\%$  during the morning, at noon and in the early afternoon, and started to decrease in the late afternoon to  $c. 30\%$  at sunset. Outside the chambers relative humidity was lowest at  $c. 15:00$  h, and was  $58\%$  on average. During nighttime respiration measurements, relative humidity in the chambers was  $73\%$  on average, compared with  $95\%$  outside the chambers.

Overall, the modifications of climatic conditions by the OTCs were quite modest and well inside the range of chamber effects reported by others (e.g. Sanders *et al.*, 1991; Leadley & Drake, 1993; Liu *et al.*, 2000; Dore *et al.*, 2003). This was true except for air humidity, which was lower than ambient in the present system, but is higher than ambient in most OTCs (e.g. Dore *et al.*, 2003). Ambient temperature was tracked rather well by the new OTC system.

**Concentration and isotope composition of  $\text{CO}_2$  during labelling**  $\text{CO}_2$  concentration and  $\delta^{13}\text{C}$  at the chamber inlet and outlet in the daytime are shown in Fig. 4. As expected,  $\text{CO}_2$  concentration at the outlet was lower than at the inlet as a result of photosynthetic  $\text{CO}_2$  uptake, and  $\delta^{13}\text{C}$  at the outlet was enriched compared with the inlet as a result of photosynthetic discrimination against  $^{13}\text{C}$ . In chamber air (reflected by the outlet observations),  $\text{CO}_2$  concentration was comparable to the ambient concentration, being  $367 \pm 6.5 \mu\text{mol mol}^{-1}$  at noon.  $\delta^{13}\text{C}$  at the chamber outlet was up to  $1\text{‰}$  more depleted in the morning and evening than during the brightest period of the day. But, as the assimilation rate was lower in the morning and evening, the contribution of these periods with more depleted  $\delta^{13}\text{C}$  to the total amount of assimilated tracer was small. The assimilation-weighted mean  $\delta^{13}\text{C}$  of  $\text{CO}_2$  in the OTCs was  $-46.9\text{‰}$  (while the daytime mean  $\delta^{13}\text{C}$  of ambient  $\text{CO}_2$  was  $-8.5\text{‰}$ ). SD including day-to-day variation as well as variation between the chambers was  $1.2 \mu\text{mol mol}^{-1}$  and  $0.11\text{‰}$  at the chamber inlet and  $6.5 \mu\text{mol mol}^{-1}$  and  $0.38\text{‰}$  at the chamber outlet.

#### Labelling kinetics of ecosystem respired $\text{CO}_2$

The rate of total ecosystem respiration,  $F_{\text{resp}}$ , measured online in the field, was  $6.7 \pm 0.3 \mu\text{mol m}^{-2} \text{s}^{-1}$  on average ( $\pm$  SE);

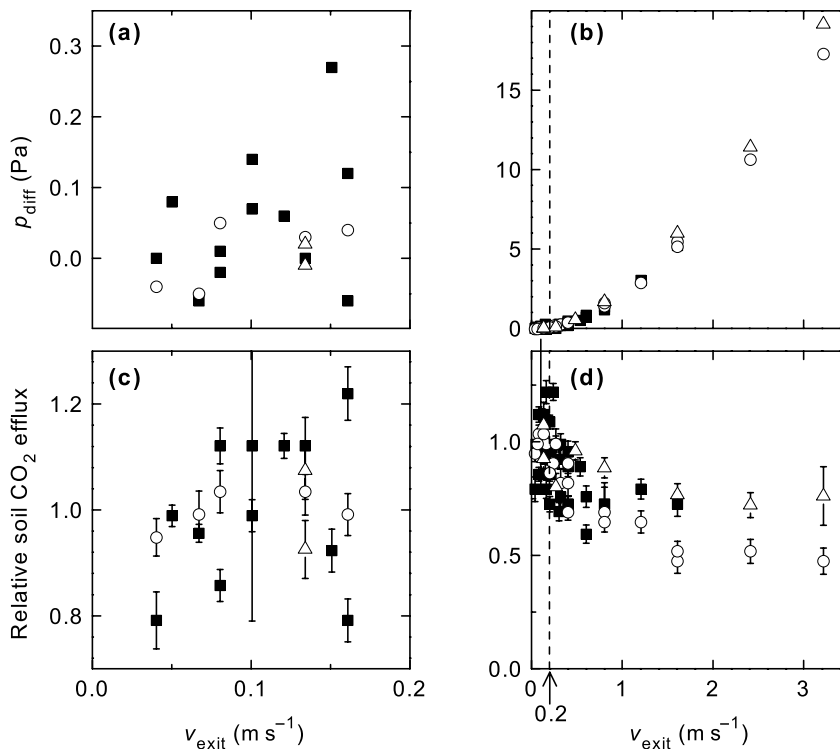


**Fig. 3** (a, b) Overpressure and (c, d) relative soil CO<sub>2</sub> efflux observed inside a chamber enclosing a grassland canopy, but with aboveground vegetation clipped and removed. Different symbols indicate different days of observation (squares, 20 September 2005; circles, 22 September 2005; triangles, 13 October 2005). Relative soil CO<sub>2</sub> efflux is related to the mean soil CO<sub>2</sub> efflux for  $v_{\text{exit}}$  (the velocity of air exiting through the top) < 0.2 m s<sup>-1</sup> to facilitate comparison of measurements from different days with different absolute efflux rates. (a) and (c) expand the range of  $v_{\text{exit}}$  < 0.2 m s<sup>-1</sup>.

$n = 68$ ) during the whole labelling experiment.  $\delta^{13}\text{C}$  of ecosystem respired CO<sub>2</sub> ( $\delta_{\text{resp}}$ ) is shown in Fig. 5a. In the unlabelled ecosystem (before the start of labelling),  $\delta_{\text{resp}}$  was  $-26.7 \pm 0.2\text{‰}$  ( $\pm$  SE;  $n = 4$ ). Labelling with <sup>13</sup>C-depleted CO<sub>2</sub> caused a decrease of  $\delta_{\text{resp}}$ . This decrease was fast during the first few days of labelling, but then slowed until  $\delta_{\text{resp}}$  became almost constant at  $c. -44\text{‰}$  in the second week of labelling. The time-course of  $\delta_{\text{resp}}$  was translated into  $f_{\text{new}}$ , the fraction of labelled C in respired C, using Eqns 3 and 4 (Fig. 5b) and a  $\Delta$  of 18.7‰, as determined by gas exchange measurements before labelling (Eqn 5).

Reference values of  $\delta_{\text{resp}}$  measured in the laboratory-based gas exchange system tended to be 1–2‰ more depleted than *in situ* observed values, independent of the duration of labelling. Translation of  $\delta_{\text{resp}}$  to  $f_{\text{new}}$  is relative to the unlabelled system for both measurement methods, and so eliminated the offset between laboratory and *in situ* measured  $\delta_{\text{resp}}$ . Accordingly,  $f_{\text{new}}$  from (laboratory) reference and *in situ* measurements agreed within measurement uncertainty (Fig. 5b). Extreme rainfall occurred on the last 2 d of the experiment ( $c. 60 \text{ mm d}^{-1}$ ), which caused saturation of soil with water even inside the chambers. Measurements accomplished in that period were ‘noisy’ and not considered in the following analysis of the labelling kinetics.

The kinetics of  $f_{\text{new}}$  was approximated ( $r^2 = 0.97$ ) with a two-source model, which included one source that obeyed first-order labelling kinetics (source A) and another source that did not release label during the 14-d-long continuous

labelling (source B). This was represented by the following single-exponential function:

$$f_{\text{new}}(t) = a(1 - e^{-bt}) \quad \text{Eqn 6}$$

in which  $t$  denotes labelling duration. The fit parameter  $a$  gives the fractional contribution of source A to total ecosystem respiration, and the (fitted) rate constant  $b$  describes the turnover of source A. The fractional contribution of source B to ecosystem respiration is given by  $1 - a$ . Simpler models yielded inferior fits to the  $f_{\text{new}}$  data, whereas double or even higher exponential functions did not improve the goodness of the fit (data not shown). Thus, Eqn 6 represented the simplest model that contained all essential kinetic features of the supply system feeding ecosystem respiration (in other words, this model contained all necessary and no (statistically) redundant features). The half-life ( $T_{1/2}$ ) of source A was obtained as  $T_{1/2} = \log_e(2)/b$  and was 2.6 d (Table 2). The contributions of the two sources to ecosystem respiration were very similar: source A contributed 48% and source B 52%.

## Discussion

### Labelling performance

The new apparatus provided a strong, uniform and constant <sup>13</sup>CO<sub>2</sub>/<sup>12</sup>CO<sub>2</sub> labelling signal throughout a 16-d-long labelling experiment of a grassland ecosystem under near-natural

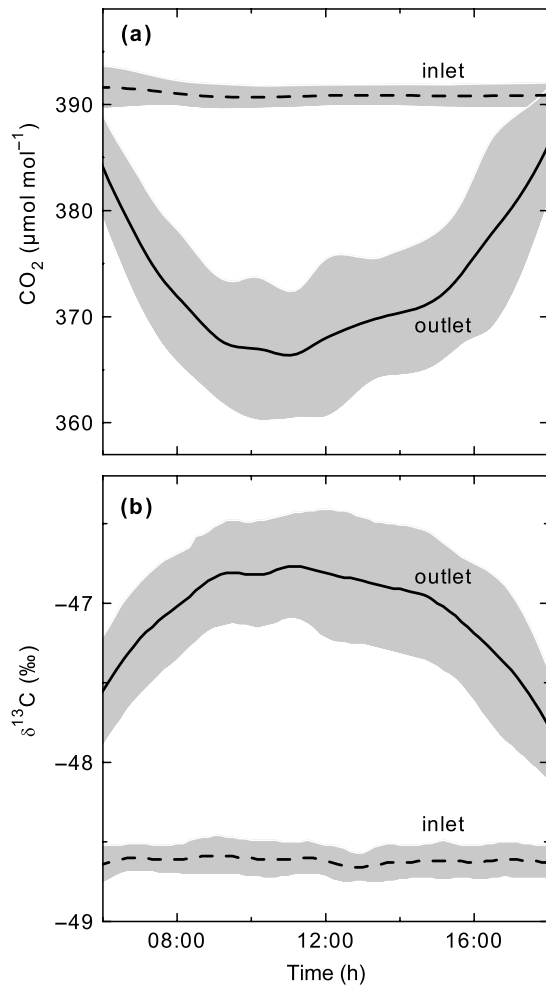


**Fig. 4** Average diurnal cycle of (a) CO<sub>2</sub> concentration and (b) δ<sup>13</sup>C of CO<sub>2</sub> in air at the chamber inlet (dashed lines) and outlet (solid lines) during the light period. Lines indicate the mean of the four open-top chambers during the 2-wk-long labelling experiment, and shaded areas indicate SD including day-to-day variation as well as variation between the different chambers.

**Table 2** Parameters characterizing tracer kinetics of ecosystem respired CO<sub>2</sub>, measured online in the field

Fit parameter (Eqn 6)	Fit parameter value (± SE)
<i>a</i>	0.48 ± 0.015
1 - <i>a</i>	0.52 ± 0.015
<i>T</i> <sub>1/2</sub> (d)	2.6 ± 0.2

*a*, fractional contribution of source A to total ecosystem respiration; *T*<sub>1/2</sub> = log<sub>e</sub>(2)/*b*, half-life of source A.

environmental conditions: the δ<sup>13</sup>C of CO<sub>2</sub> in the OTC was maintained at -46.9‰, ~38‰ less than that of ambient CO<sub>2</sub>, with a precision (SD) of 0.4‰ for variations across the labelling experiment duration and all OTCs; CO<sub>2</sub> concentration was maintained at 367 ± 6.5 μmol mol<sup>-1</sup> at midday; and mixing of CO<sub>2</sub> inside the OTC was spatially uniform and near-instantaneous.

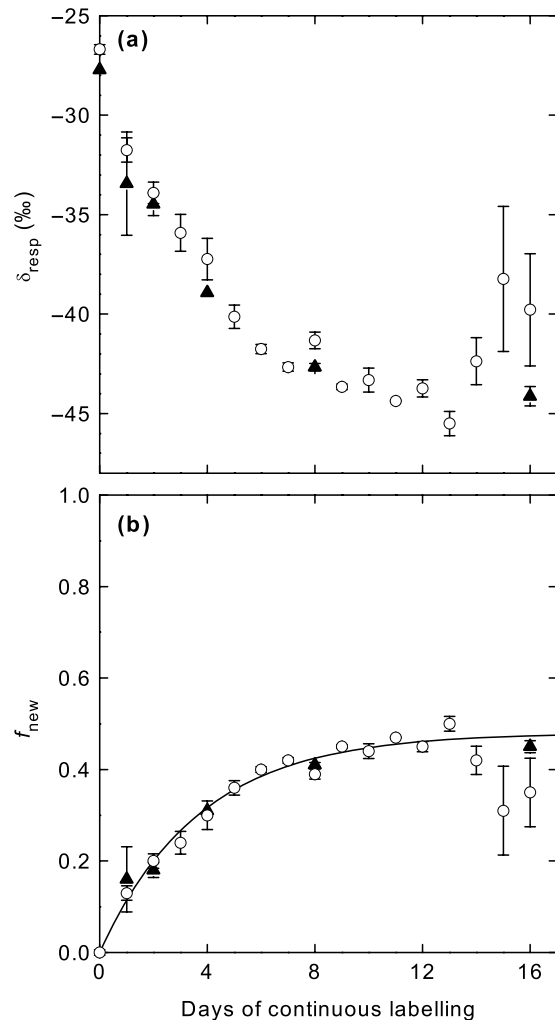


**Fig. 5** Labelling kinetics of ecosystem respired CO<sub>2</sub>. (a) δ<sup>13</sup>C of ecosystem respiration and (b) fraction of labelled carbon (C) in ecosystem respired C during a 16-d-long continuous labelling experiment. Respiration measurements were made at night. Open circles, online measurements in the field; closed triangles, laboratory-based reference measurements on excised soil + vegetation blocks under controlled conditions. Error bars indicate SE (*n* = 2–9). The line in (b) is the fit according to Eqn 6. Extreme rainfall occurred on days 15 and 16. Data from these days were not included in the fit.

The small variation in the concentration and isotopic composition of CO<sub>2</sub> supplied to the chambers is a measure of the combined precision of the gas mixing and the measurement device (infrared gas analyser and mass spectrometer) and was within the range reported by Schnyder *et al.* (2004). The considerably higher variation at the chamber outlet was mainly attributable to variations in assimilation rate. These variations cannot be controlled easily by the experimentalist as they depend strongly on incoming radiation, which varies diurnally and with cloudiness. Nevertheless, the variations were small in comparison to the labelling signal, which was ~100 times larger than the labelling precision, as a result of the

high air flow through the OTCs. Air incursion also contributed to the variations at the chamber outlet, but these variations were negligible compared with the variations caused by assimilation. Furthermore, near-instantaneous mixing led to homogeneous tracer distribution inside the chamber. In consequence, sampling of chamber outlet air could be performed anywhere inside the well-mixed chamber, as the conditions inside the chamber were uniform.

### *In situ* observation of tracer kinetics in respired CO<sub>2</sub>

The labelling kinetics of respiratory CO<sub>2</sub> was measured accurately and precisely by the OTC-based online <sup>13</sup>CO<sub>2</sub>/<sup>12</sup>CO<sub>2</sub> gas exchange system, as confirmed by the reference measurements of  $f_{\text{new}}$ . In the reference system cuvettes, the excised soil + vegetation blocks were completely enclosed and hence all respired CO<sub>2</sub> was captured by the measurements. The concordance of  $f_{\text{new}}$  values obtained with both methods provides convincing evidence that the new OTC method captured the unbiased isotopic signal of total ecosystem respiration, despite the fact that the OTCs were open at the bottom. The high accuracy and precision were related to two main features of chamber design and operation conditions: the effective prevention of ambient air incursion into the chamber by the buffered vent of the OTCs, and the absence of pressure effects on soil CO<sub>2</sub> efflux during nighttime respiration measurements. In windy conditions (wind speeds of 2–3 m s<sup>-1</sup> during nighttime measurements), air incursions produced an air<sub>amb</sub>/air<sub>chamber</sub> ratio of 0.0015, which meant a change of 0.05‰ of δ<sub>out</sub>. This effect translated into a 0.5‰ change of δ<sub>resp</sub> and a 1% decrease of  $f_{\text{new}}$ . In calm conditions (which prevailed during most nights), less ambient air was blown into the OTCs. Simultaneously, a given amount of ambient air entering the chamber brought a larger quantity of ‘contaminating’ CO<sub>2</sub>, as a result of the larger nighttime build-up of ambient CO<sub>2</sub> concentration. Nevertheless, the total impact of air incursion on  $f_{\text{new}}$  was < 1% on calm nights. According to Baldocchi *et al.* (1989) the efficiency of preventing air incursion into OTCs is dependent on the relationship between chamber volume size and effective eddy size. In the present OTCs the buffer volume had a height of 0.2 m, which suppressed the formation of a roll vortex in the OTCs at the prevailing effective eddy size (0.35 m; calculated according to Baldocchi *et al.*, 1989).

Notably, there was a systematic 1–2‰ offset between δ<sub>resp</sub> values measured in the two gas exchange systems. This offset was related to the fact that δ<sub>resp</sub> decreased during the course of the night (data not shown) and laboratory-based (reference) measurements were carried out several hours after the on-site measurements. The effect of such changes on the labelling kinetics (i.e. the time-course of  $f_{\text{new}}$ ) was eliminated by accounting for the diurnal changes by determining δ<sub>resp</sub> of the nonlabelled ecosystem in the two measurement systems. No other factors affecting the δ offset between the two systems

were found; cross-calibration of the two systems ensured that δ<sup>13</sup>C measurements were unbiased.

Estimation of  $f_{\text{new}}$  was based on the assumption that <sup>13</sup>C discrimination during photosynthesis (Δ) was the same inside and outside the OTCs and did not vary over time. Almost certainly, this assumption was not exactly true. However, the sensitivity of  $f_{\text{new}}$  to variations in Δ was small: a 1‰ increase/decrease in Δ caused a 1% decrease/increase in  $f_{\text{new}}$ . Measurements of community-level Δ in a large range of weather conditions and soil water availabilities indicated that Δ did not vary by more than ±1‰ at the experimental site (Schnyder *et al.*, 2006).

### Tracer kinetics reveals two sources supplying respiration

The labelling kinetics showed that ecosystem respiration was fuelled by two distinct sources: one was closely connected to current photosynthetic activity, and the other was supplied by substrate that was not labelled within the 2-wk-long labelling period. A source is defined here as a cluster of biochemical compounds distributed among different organisms, which exhibited the same (or a similar) pattern of tracer incorporation (Lehmeier *et al.*, 2008). Thus, although there was a diversity of metabolic activities in the ecosystem, each (major) activity could be assigned to one of two substrate clusters, which differed in C age.

Source A, which was turned over by photosynthesis with a half-life of *c.* 2.6 d, must have included most (if not all) of autotrophic respiration. Autotrophic respiration is supplied by nonstructural components of plant biomass, which are turned over relatively rapidly by current photosynthate. In a controlled environment study, Lehmeier *et al.* (2008) found a half-life of *c.* 2 d for the total substrate pool feeding root and shoot respiration of *Lolium perenne*, a main component of the grassland ecosystem. In that study, root and shoot respiration exhibited near-identical labelling kinetics. Moreover, only *c.* 5% of root and shoot respiration was supplied by substrates older than 10 d, showing that long-term reserves/storage pools were relatively unimportant substrates of autotrophic respiration. In another study on the same species, 50% of the root exudates were turned over by current photosynthate within 4.5 d (Thornton *et al.*, 2004). In addition, it has been shown that arbuscular mycorrhizal mycelia can provide a fast pathway for respiratory release of current photosynthate, releasing C within hours to days after its assimilation under field conditions (Johnson *et al.*, 2002; see also Heinemeyer *et al.*, 2006 and Hawkes *et al.*, 2008). Furthermore, the observed half-life of source A compares reasonably well with the mean age of 5–8 d (corresponding to a half-life of 3.5–5.5 d) determined for autotrophically respired C, including respiration from root-associated microbes, in a California mountain grassland ecosystem (Carbone & Trumbore, 2007). All these components (shoot, root and rhizosphere respiration) must have contributed to the respiratory activity associated with source A, and the sum

of these activities constitutes autotrophic respiration (Hanson *et al.*, 2000; Subke *et al.*, 2006; Trumbore, 2006; but see also Chapin *et al.*, 2006 and Kuzyakov, 2006). Therefore, we regard the total activity of source A (about half of ecosystem respiration) as a measure of autotrophic respiration.

The other source (source B) did not release any label within the 2-wk-long labelling period, showing that it was supplied by pools with very slow turnover ( $\geq$  months) or that the release of the substrate from the pools occurred only after an extensive lag (delay). Leaf and root litter are the main substrates for heterotrophic respiration (Ryan & Law, 2005), as structural biomass is the C source for the various heterotrophic pathways including decomposition via soil organic carbon. C incorporated into structural biomass of leaf and root tissues is protected from respiratory consumption until the end of the tissues' life span, when it passes on to the litter fraction and becomes available for decomposers. Leaf life span of the dominant species at the study site was *c.* 27 d (I. Schleip, unpublished data). Others have observed leaf life spans of 22–95 d in a range of grassland species and sites (Diemer *et al.*, 1992; Lemaire & Chapman, 1996; Ryser & Urbas, 2000). The life span of grass roots is even longer, in the order of months (Van der Krift & Berendse, 2002). Thus, all in all, only a very small amount of labelled plant material had been turned into litter and soil organic matter during the labelling experiment. Therefore, all (heterotrophic) processes decomposing old (nonlabelled) dead plant material and soil organic matter were pooled in source B. Resolving further functional components of source B would require extension of the labelling duration.

In conclusion, this work presents a new OTC-based continuous  $^{13}\text{CO}_2/^{12}\text{CO}_2$  labelling and gas exchange measurement system for studies of C allocation and turnover of grassland ecosystems, including the assessment of respiratory substrate pool kinetics. Tests of chamber performance and optimization of OTC design and operation conditions minimized common artefacts such as ambient air incursion and suppression of soil  $\text{CO}_2$  efflux, and ensured a high accuracy and precision of daytime  $^{13}\text{CO}_2/^{12}\text{CO}_2$  labelling and nighttime respiration measurements. The method is well suited for labelling studies at any  $\text{CO}_2$  concentration, from subambient to elevated  $\text{CO}_2$ , as was also demonstrated by Lehmeier *et al.* (2005) in a controlled environment system employing the same gas exchange and labelling methodology. We suggest that the two kinetically distinct sources of respiration detected in this work at ambient  $\text{CO}_2$  concentration represent the autotrophic (including rhizosphere) and heterotrophic components of grassland ecosystem respiration.

## Acknowledgements

The members of the Lehrstuhl für Grünlandlehre (Technische Universität München) are gratefully acknowledged for continuous support; in particular, Richard Wenzel is thanked

for expert technical assistance and Inga Schleip and Christoph Lehmeier for valuable discussions. Dave Bowling and Andrew Moyes are thanked for helpful discussion. The investigations were partially supported by SFB 607.

## References

- Atkins GL. 1969. *Multicompartment models in biological systems*. London, UK: Methuen & Co. Ltd.
- Bahn M, Schmitt M, Siegwolf R, Richter A, Brüggemann N. 2009. Does photosynthesis affect grassland soil-respired  $\text{CO}_2$  and its carbon isotopic composition on a diurnal timescale? *New Phytologist* 182: 451–460.
- Baldocchi DD, White R, Johnston JW. 1989. A wind-tunnel study to design large, open-top chambers for whole-tree pollutant exposure experiments. *Japca – The Journal of the Air & Waste Management Association* 39: 1549–1556.
- Carbone MS, Czimczik CI, McDuffee KE, Trumbore SE. 2007. Allocation and residence time of photosynthetic products in a boreal forest using a low-level  $^{14}\text{C}$  pulse-chase labeling technique. *Global Change Biology* 13: 466–477.
- Carbone MS, Trumbore SE. 2007. Contribution of new photosynthetic assimilates to respiration by perennial grasses and shrubs: residence times and allocation patterns. *New Phytologist* 176: 124–135.
- Chapin FS, Woodwell GM, Randerson JT, Rastetter EB, Lovett GM, Baldocchi DD, Clark DA, Harmon ME, Schimel DS, Valentini R *et al.* 2006. Reconciling carbon-cycle concepts, terminology, and methods. *Ecosystems* 9: 1041–1050.
- Deléens E, Pavlides D, Queiroz O. 1983. Natural  $^{13}\text{C}$  abundance as a tracer for the determination of leaf matter turn-over in C3 plants. *Physiologie Vegetale* 21: 723–729.
- Diemer M, Körner C, Prock S. 1992. Leaf life spans in wild perennial herbaceous plants – a survey and attempts at a functional interpretation. *Oecologia* 89: 10–16.
- Dore S, Hymus GJ, Johnson DP, Hinkle CR, Valentini R, Drake BG. 2003. Cross validation of open-top chamber and eddy covariance measurements of ecosystem  $\text{CO}_2$  exchange in a Florida scrub-oak ecosystem. *Global Change Biology* 9: 84–95.
- Fang C, Moncrieff JB. 1998. An open-top chamber for measuring soil respiration and the influence of pressure difference on  $\text{CO}_2$  efflux measurement. *Functional Ecology* 12: 319–325.
- Geiger DR. 1980. Measurement of translocation. *Methods in Enzymology* 69: 561–571.
- Hanson PJ, Edwards NT, Garten CT, Andrews JA. 2000. Separating root and soil microbial contributions to soil respiration: A review of methods and observations. *Biogeochemistry* 48: 115–146.
- Hawkes CV, Hartley IP, Ineson P, Fitter AH. 2008. Soil temperature affects carbon allocation within arbuscular mycorrhizal networks and carbon transport from plant to fungus. *Global Change Biology* 14: 1181–1190.
- Heinemeyer A, Ineson P, Ostle N, Fitter AH. 2006. Respiration of the external mycelium in the arbuscular mycorrhizal symbiosis shows strong dependence on recent photosynthates and acclimation to temperature. *New Phytologist* 171: 159–170.
- Högberg P, Högberg MN, Göttlicher SG, Betson NR, Keel SG, Metcalfe DB, Campbell C, Schindlbacher A, Hurry V, Lundmark T *et al.* 2008. High temporal resolution tracing of photosynthate carbon from the tree canopy to forest soil microorganisms. *New Phytologist* 177: 220–228.
- Högberg P, Read DJ. 2006. Towards a more plant physiological perspective on soil ecology. *Trends in Ecology & Evolution* 21: 548–554.
- Jacquez J. 1996. *Compartmental analysis in biology and medicine*. Amsterdam, the Netherlands: Elsevier Publishing Company.

- Johnson D, Leake JR, Ostle N, Ineson P, Read DJ. 2002. *In situ*  $^{13}\text{CO}_2$  pulse-labelling of upland grassland demonstrates a rapid pathway of carbon flux from arbuscular mycorrhizal mycelia to the soil. *New Phytologist* 153: 327–334.
- Kanemasu ET, Powers WL, Sij JW. 1974. Field chamber measurements of  $\text{CO}_2$  flux from soil surface. *Soil Science* 118: 233–237.
- Kuzyakov Y. 2006. Sources of  $\text{CO}_2$  efflux from soil and review of partitioning methods. *Soil Biology & Biochemistry* 38: 425–448.
- Leadley PW, Drake BG. 1993. Open top chambers for exposing plant canopies to elevated  $\text{CO}_2$  concentration and for measuring net gas-exchange. *Vegetatio* 104: 3–15.
- Lehmeier CA, Lattanzi FA, Schäufele R, Wild M, Schnyder H. 2008. Root and shoot respiration of Perennial Ryegrass are supplied by the same substrate pools: assessment by dynamic  $^{13}\text{C}$  labeling and compartmental analysis of tracer kinetics. *Plant Physiology* 148: 1148–1158.
- Lehmeier CA, Schäufele R, Schnyder H. 2005. Allocation of reserve-derived and currently assimilated carbon and nitrogen in seedlings of *Helianthus annuus* under subambient and elevated  $\text{CO}_2$  growth conditions. *New Phytologist* 168: 613–621.
- Lemaire G, Chapman D. 1996. Tissue flows in grazed plant communities. In: Hodgson J, Illius AW, eds. *The ecology and management of grazing systems*. Wallingford, UK: Cab International, 3–36.
- Liu L, Hoogenboom G, Ingram KT. 2000. Controlled-environment sunlit plant growth chambers. *Critical Reviews in Plant Sciences* 19: 347–375.
- Livingston GP, Hutchinson GL. 1995. Enclosure-based measurement of trace gas exchange: applications and sources of error. In: Matson PA, Harriss RC, eds. *Biogenic trace gases: Measuring emissions from soil and water*. Oxford, UK: Blackwell Science, 14–51.
- Lötscher M, Klumpp K, Schnyder H. 2004. Growth and maintenance respiration for individual plants in hierarchically structured canopies of *Medicago sativa* and *Helianthus annuus*: the contribution of current and old assimilates. *New Phytologist* 164: 305–316.
- Lund CP, Riley WJ, Pierce LL, Field CB. 1999. The effects of chamber pressurization on soil-surface  $\text{CO}_2$  flux and the implications for NEE measurements under elevated  $\text{CO}_2$ . *Global Change Biology* 5: 269–281.
- Meharg AA. 1994. A critical-review of labeling techniques used to quantify rhizosphere carbon-flow. *Plant and Soil* 166: 55–62.
- Nogues S, Tcherkez G, Cornic G, Ghashghaie J. 2004. Respiratory carbon metabolism following illumination in intact french bean leaves using  $^{13}\text{C}/^{12}\text{C}$  isotope labeling. *Plant Physiology* 136: 3245–3254.
- Ostle N, Ineson P, Benham D, Sleep D. 2000. Carbon assimilation and turnover in grassland vegetation using an *in situ*  $^{13}\text{CO}_2$  pulse labelling system. *Rapid Communications in Mass Spectrometry* 14: 1345–1350.
- Ratcliffe RG, Shachar-Hill Y. 2006. Measuring multiple fluxes through plant metabolic networks. *Plant Journal* 45: 490–511.
- Ryan MG, Law BE. 2005. Interpreting, measuring, and modeling soil respiration. *Biogeochemistry* 73: 3–27.
- Ryle GJA, Cobby JM, Powell CE. 1976. Synthetic and maintenance respiratory losses of  $^{14}\text{CO}_2$  in unicum barley and maize. *Annals of Botany* 40: 571–586.
- Ryser P, Urbas P. 2000. Ecological significance of leaf life span among Central European grass species. *Oikos* 91: 41–50.
- Sanders GE, Clark AG, Colls JJ. 1991. The influence of open-top chambers on the growth and development of field bean. *New Phytologist* 117: 439–447.
- Schnyder H, Schäufele R, Lötscher M, Gebbing T. 2003. Disentangling  $\text{CO}_2$  fluxes: direct measurements of mesocosm-scale natural abundance  $^{13}\text{CO}_2/^{12}\text{CO}_2$  gas exchange,  $^{13}\text{C}$ -discrimination, and labelling of  $\text{CO}_2$  exchange flux components in controlled environments. *Plant, Cell & Environment* 26: 1863–1874.
- Schnyder H, Schäufele R, Wenzel R. 2004. Mobile, outdoor continuous-flow isotope-ratio mass spectrometer system for automated high-frequency  $^{13}\text{C}$ - and  $^{18}\text{O}$ - $\text{CO}_2$  analysis for Keeling plot applications. *Rapid Communications in Mass Spectrometry* 18: 3068–3074.
- Schnyder H, Schwertl M, Auerswald K, Schäufele R. 2006. Hair of grazing cattle provides an integrated measure of the effects of site conditions and inter-annual weather variability on  $\delta^{13}\text{C}$  of temperate humid grassland. *Global Change Biology* 12: 1–15.
- Subke JA, Inglima I, Cotrufo MF. 2006. Trends and methodological impacts in soil  $\text{CO}_2$  efflux partitioning: A metaanalytical review. *Global Change Biology* 12: 921–943.
- Thornton B, Paterson E, Midwood AJ, Sim A, Pratt SM. 2004. Contribution of current carbon assimilation in supplying root exudates of *Lolium perenne* measured using steady-state  $^{13}\text{C}$  labelling. *Physiologia Plantarum* 120: 434–441.
- Trumbore SE. 2006. Carbon respired by terrestrial ecosystems – recent progress and challenges. *Global Change Biology* 12: 141–153.
- Van der Krift TAJ, Berendse F. 2002. Root life spans of four grass species from habitats differing in nutrient availability. *Functional Ecology* 16: 198–203.

## Supporting Information

Additional supporting information may be found in the online version of this article.

**Fig. S1** Schematic diagram of the laboratory-based open  $^{13}\text{CO}_2/^{12}\text{CO}_2$  gas exchange cuvette, adapted for reference measurements of the isotopic composition of ecosystem respiration.

**Fig. S2** Half-lives of  $\text{CO}_2$  concentration changes in chamber air, following abrupt changes in  $\text{CO}_2$  concentration of the incoming air.

**Fig. S3** Air temperature, relative humidity and photosynthetic photon flux density (PPFD) during the labelling experiment.

Please note: Wiley-Blackwell are not responsible for the content or functionality of any supporting information supplied by the authors. Any queries (other than missing material) should be directed to the *New Phytologist* Central Office.